

Beyond the Core+ $n+n$ Model Based on the Complex Scaling Method

Kiyoshi KATŌ,^{1,*} Takayuki MYO,^{1,**} Shigeyoshi AOYAMA^{2,***}
and Kiyomi IKEDA^{3,†}

¹*Division of Physics, Graduate School of Science, Hokkaido University,
Sapporo 060-0810, Japan*

²*Information Processing Center, Kitami Institute of Technology,
Kitami 090-8507, Japan*

³*RI-Beam Science Laboratory, RIKEN, Wako 351-0198, Japan*

(Received February 5, 2002)

With a new framework beyond the simple core+ $n+n$ model, we study neutron halo nuclei, taking into account a dynamical coupling between configurations of the core cluster and valence neutrons. It is shown that such a dynamical coupling is very important in ^{10}Li and ^{11}Li though less important in ^6He . We apply the new core+neutrons model to $^9\text{Li}+n$ and $^9\text{Li}+n+n$ where the ^9Li core includes $J^\pi = 0^+$ neutron pairing correlations. In this new model, we solve the coupled channel OCM equation, and discuss the energy degeneracy of s - and p -wave neutron orbits in ^{10}Li and the halo structure in ^{11}Li . In those calculations, the complex scaling method is extensively used to solve two-body and three-body resonances together with bound states in the same framework. The complex scaling method is also applied to the three-body Coulomb breakup by means of the extended completeness relation. This method is applied to the breakup reactions of ^6He and ^{11}Li .

§1. Introduction

To understand the exotic properties of ^{11}Li and ^6He , the core+ $n+n$ model¹⁴⁾ has been extensively studied where a frozen configuration cluster has been assumed for the core cluster. This assumption for the $^4\text{He}+n+n$ model is shown to work well in describing not only the ground states but also the excited resonant states in ^6He .¹⁾ However, the $^9\text{Li}+n+n$ model, where the simple shell model configuration has been assumed for the ^9Li core, is shown to fail in explaining the binding energy of ^{11}Li .²⁾

To solve those problems of the simple core+ $n+n$ model, we propose a new framework in which we can treat the coupling between an intrinsic correlation in the core cluster and the motion of valence neutrons. As an important correlation causing the ^9Li core configuration mixing, we take into account the neutron-neutron $J^\pi = 0^+$ pairing. To ^{10}Li , the coupled channel $^9\text{Li}+n$ model with multi-configurations of ^9Li is applied and the coupling between the pairing correlation in the ^9Li core and the valence neutron motion is solved. The result shows the very strong effect of the pairing blocking on the $^9\text{Li}-n$ interaction.³⁾ The obtained $^9\text{Li}-n$ interaction provides

^{*}) E-mail: kato@nucl.sci.hokudai.ac.jp

^{**}) E-mail: myo@nucl.sci.hokudai.ac.jp

^{***}) E-mail: aoyama@nucl.sci.hokudai.ac.jp

[†]) E-mail: k-ikeda@postman.riken.go.jp

us with a virtual s -wave resonance⁴⁾ in ^{10}Li , and improves the binding energy of the $^9\text{Li}+n+n$ system.

However, we also show that a large amplitude of s -wave valence neutrons, which is an important origin of the halo structure in ^{11}Li , cannot be explained only by the Pauli-blocking effect on the pairing correlation. In order to solve this difficulty, we introduce a long-range potential tail in the $^9\text{Li}-n$ interaction. This long-range potential tail is considered to come from the Pauli principle between valence and core neutron-pair. In this study, the long-range potential tail of $^9\text{Li}-n$ is treated by a Yukawa-form with a phenomenological parameter. The observed ground state properties of ^{11}Li are shown to be well explained in this model.

Studies of resonances are indispensable to understand the unique properties of drip-line nuclei. Although it is easy to solve resonances of two-body systems, resonances of three-body systems such as the so-called Borromean systems⁵⁾ are not simple, because various kinds of open channel structures appear. For example, $^6\text{He}=^4\text{He}+n+n$ being a typical Borromean system, has the thresholds of $[^4\text{He}+n]_{\text{res}} + n$ with complex threshold energies appearing above the three-body threshold of $^4\text{He}+n+n$. Therefore, the continuum states of ^6He consist of three-body components of $^4\text{He}+n+n$ and quasi-two-body ones of $[^4\text{He}+n]_{\text{res}} + n$, where the $^4\text{He}+n$ system has two resonances of $3/2^-$ and $1/2^-$. In this paper, it is shown that the complex scaling method⁶⁾ is very useful for studying loosely bound states, resonances and continuum states in a unified way.⁷⁾ Using the complex scaling method, we extensively study ^6He and ^{11}Li based on the core+ $n+n$ microscopic three-body cluster model.⁸⁾

§2. A new core-plus-neutrons model for neutron halo nuclei

The core-plus-neutrons model expresses a double structure of the strong and the weak binding parts by a core cluster and valence neutrons of a halo nucleus, respectively.⁹⁾⁻¹¹⁾ In this model for a halo nucleus A , the Hamiltonian is given by

$$H(A) = H_c(C) + H_n + H_{\text{int}}, \quad (2.1)$$

where H_c and H_n are Hamiltonians for the core cluster C and the valence neutrons, respectively, and H_{int} describes the coupling between different parts. The wave function for the Hamiltonian H can be written as

$$\Psi(A) = \sum_i \mathcal{A} \{ \Phi_i(C) \chi_i(N) \}, \quad (2.2)$$

where the wave function $\Phi_i(C)$ is a configuration of the core cluster C .

The relative motion, $\chi_i(N)$, between the core cluster and the valence neutrons is solved on the basis of recent developments in few-body problems, where the antisymmetrization is treated by the orthogonality condition model (OCM)¹²⁾ for the Pauli forbidden states. In the dynamics between core cluster and valence neutrons, important correlations are described by the mean field dominantly coming from the core-neutron interaction and by the pairing correlation from the neutron-neutron

interaction. The former correlation has been found to be expressed by the cluster orbital shell model (COSM)¹³⁾ and the latter by the extended-cluster model (ECM).^{14),15)} For the relative coordinates in COSM (V-type) and ECM (T-type) shown in Fig. 1, the relative wave functions are expressed in the following hybrid-TV model of a linear combination of COSM (V-type) and ECM (T-type) basis wave functions:

$$\chi_{IM}(N) = \chi_{IM}(V) + \chi_{IM}(T), \quad (2.3)$$

where

$$\chi_{IM}(V) = \sum_{l_1 j_1 l_2 j_2} \mathcal{A} [\phi_{l_1 j_1}(\vec{\eta}_1) \phi_{l_2 j_2}(\vec{\eta}_2)]_{IM}, \quad (2.4)$$

$$\chi_{IM}(T) = \sum_{\lambda_1 \lambda_2 LS} \mathcal{A} \left[[u_{\lambda_1}(\vec{r}) u_{\lambda_2}(\vec{R})]_L [s_{1/2}(1) s_{1/2}(2)]_S \right]_{IM}. \quad (2.5)$$

§3. ${}^6\text{He}$: Beyond the ${}^4\text{He}+n+n$ model

Assuming a single shell model configuration for the core-cluster, we apply the ${}^4\text{He}+n+n$ model to ${}^6\text{He}$.¹⁾ Here, the ${}^4\text{He}$ core configuration is assumed to be the double-closed s -shell wave function. We employ the KKNN-potential¹⁶⁾ for ${}^4\text{He}-n$ and the Minnesota potential¹⁷⁾ for $n-n$, both of which well describe the observed properties of the two-body systems. The result of the binding energy calculations is shown in Fig. 1, where the convergence of COSM and hybrid-TV model calculations is compared. In COSM, the convergence is very slow for the channel number $[n]=[(l_n j_n)^2]_{J\pi=0^+}$. On the other hand, when we add $[l=0, L=0]_{J\pi=0^+}$ of ECM to the hybrid-TV model, we obtain a very rapid convergence. This result indicates that the pairing correlation between valence neutrons gives a large contribution to the binding of ${}^4\text{He}+n+n$.

The converged binding energy is 0.784 MeV,¹⁾ which is underbinding by about 200 keV in comparison with experimental value (0.975 MeV). This shortage is not so large, and an effect from various core-configurations is expected to be treated in a

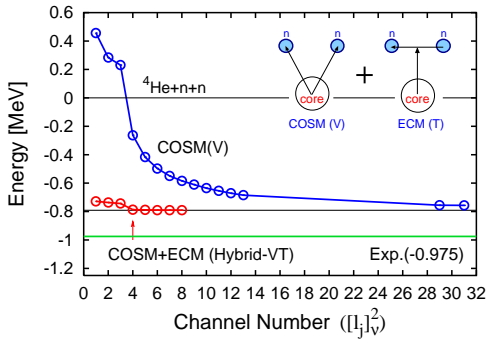


Fig. 1. Binding energy convergence of COSM and hybrid-TV model calculations of the ${}^4\text{He}+n+n$ system.

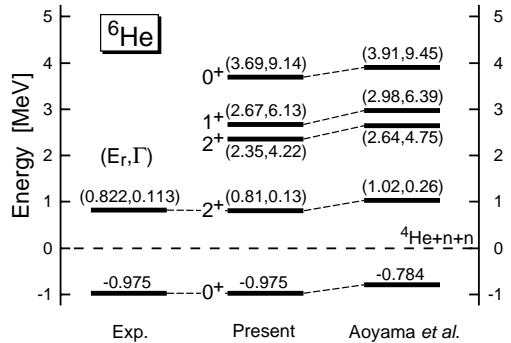


Fig. 2. Energy levels of ${}^6\text{He}$.

perturbative way. Here, we try to solve this underbinding problem by introducing an effective three-body interaction: $v_{\alpha nn}^3(\eta_1, \eta_2) = V_3 \exp\{-\nu_3(\eta_1^2 + \eta_2^2)\}$, where V_3 and ν_3 are parameters determined in order to reproduce the binding energy and the r.m.s. matter radius of ${}^6\text{He}$.⁸⁾ Applying the complex scaling method^{1), 6)} to this model, we obtain the excited resonant states of ${}^6\text{He}$, as shown in Fig. 2. Levels on the right-hand side are the results of calculation without the three-body interaction by Aoyama et al.¹⁾ Although there is not a large difference in results between with and without three-body interactions, we can see that the resonance energies and the resonance width of the 2^+ state are slightly improved. This result with the three-body interaction model, which well reproduces the binding energy and the resonance position observed in ${}^6\text{He}$, is used later in analyzing the three-body continuum structure in association with the Coulomb breakup reaction data.

Through these calculations, we can confirm that the ${}^4\text{He}+n+n$ model with the single core configuration works rather well in description of ${}^6\text{He}$. However, the ${}^9\text{Li}+n+n$ model with a single core configuration gives the binding energy underestimated by about 1 MeV.²⁾ The value is so large that we cannot treat the internal degrees of freedom in the ${}^9\text{Li}$ core in a perturbational manner.

§4. Coupled channel core+neutrons model for ${}^{10}\text{Li}$ and ${}^{11}\text{Li}$

4.1. Pauli blocking effect on the ${}^9\text{Li}-n$ interaction

We apply our core+neutrons model to ${}^{10}\text{Li}$ and ${}^{11}\text{Li}$, where we do not assume the single closed shell configuration for the ${}^9\text{Li}$ core. In the previous calculations,²⁾ we have already learned that the valence neutrons above the ${}^9\text{Li}$ core have strong pairing correlations. Accordingly, we assume that the neutron $J^\pi = 0^+$ pairing correlation is dominant in the ${}^9\text{Li}$ core. Under the assumption of the $J^\pi = 0^+$ pairing correlation, the wave function of the ${}^9\text{Li}$ cluster is expressed as³⁾

$$\Phi_{gr}({}^9\text{Li}) = \alpha_0\Phi(C_0) + \alpha_1\Phi(C_1) + \alpha_2\Phi(C_2) + \cdots, \quad (4.1)$$

where

$$(C_0) : (0s)^4(0p_{3/2})_\pi(0p_{3/2})_\nu^4, \quad (4.2)$$

$$(C_1) : (0s)^4(0p_{3/2})_\pi(0p_{3/2})_{\nu, J_1=0}^2(0p_{1/2})_{\nu, J_2=0}^2, \quad (4.3)$$

$$(C_2) : (0s)^4(0p_{3/2})_\pi(0p_{3/2})_{\nu, J_1=0}^2(1s_{1/2})_{\nu, J_2=0}^2. \quad (4.4)$$

.....

The coefficients $\{\alpha_i; i = 0, 1, 2, \dots\}$ are determined by solving the Schrödinger equation $H_c({}^9\text{Li})\Phi_{gr}({}^9\text{Li}) = \mathcal{E}_{gr}\Phi_{gr}({}^9\text{Li})$ when the ${}^9\text{Li}$ core cluster is isolated from the valence neutrons. However, when the valence neutrons approach the ${}^9\text{Li}$ core, they depend on the motion of the valence neutrons in the ${}^9\text{Li}+n$ system.

We apply this model to ${}^{10}\text{Li} = {}^9\text{Li}+n$, and investigate the ${}^9\text{Li}-n$ interaction by solving the coupling between the pairing correlation of the ${}^9\text{Li}$ core and the relative motion of valence neutrons. When we assume three configurations of C_0 , C_1 and C_3 ,

the coupled channel equation for the relative wave function $\chi_i(r)$ is given as

$$\sum_{j=0}^2 \left\{ (T_n + V_{cn} + \lambda A_j) \delta_{ij} + h_{ij}({}^9\text{Li}) \right\} \chi_j(\vec{r}) = E \chi_i(\vec{r}), \quad (i = 0, 1, 2) \quad (4.5)$$

where we employed the orthogonality condition model (OCM).¹²⁾ The matrix elements of the internal Hamiltonian H_c for $\Phi(C_i)$ are presented by $h_{ij}({}^9\text{Li})$. The operators T_n and V_{cn} correspond to kinetic and potential energies of the relative motion between core and neutron. The operator A is the Pauli-projection one, where a parameter λ is taken large enough to project out the Pauli forbidden states at unphysical energy region. The detail explanation of this equation is given in Ref. 3). Since all the states of ${}^{10}\text{Li}$ are unbound, they are solved by applying the complex scaling method.⁶⁾

In Fig. 3, the energy spectra of ${}^{10}\text{Li}$ are shown. The experimental data are taken from Ref. 18). The coupled channel result is shown as CC in comparison with the single channel one (SC).¹⁹⁾ The SC calculation corresponds to the calculation where the frozen closed shell configuration C_0 is assumed for the ${}^9\text{Li}$ core cluster. We can see that *i)* the low lying 1^+ and 2^+ states are well reproduced by both calculations of SC and CC. However, while the SC calculation gives too large widths compared with experiments, the CC result shows a significant improvement by the Pauli blocking effect. The second characteristic result of calculations is that *ii)* four resonant states arising from the $d_{5/2}$ orbital neutron are obtained at 4~6 MeV in CC, but at 7~9 MeV in SC. Although the SC calculation predicts too high resonance energies and

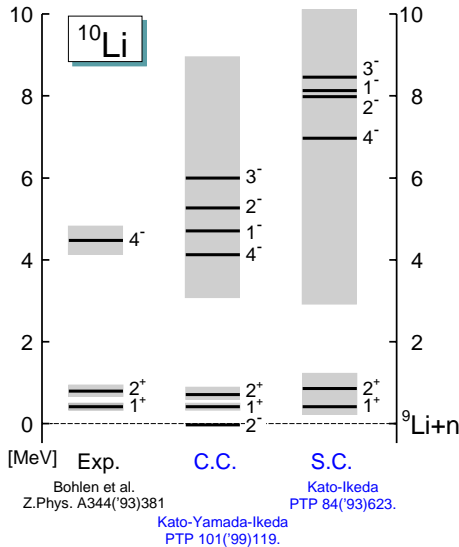


Fig. 3. Energy spectrum of ${}^{10}\text{Li}$. The experimental data are taken from Bohlen et al.,¹⁸⁾ and the theoretical ones are the single channel (S.C.)¹⁹⁾ and coupled channel (C.C.)³⁾ calculation results.

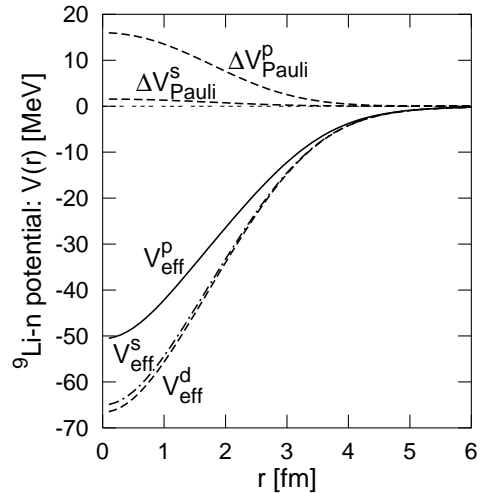


Fig. 4. Effective ${}^9\text{Li}$ - n potentials for $p_{1/2}$ -, $s_{1/2}$ - and d -orbital neutrons in the three-channel model. $\Delta V_{\text{Pauli}}^p$ and $\Delta V_{\text{Pauli}}^s$ are the repulsive potentials due to the Pauli blocking effect on $p_{1/2}$ - and $s_{1/2}$ -orbital neutrons, respectively.

too large widths for these $1^- \sim 4^-$ states, they are satisfactorily improved in the CC calculation. Furthermore, *iii*) an interesting result of CC is the prediction of the s -orbital neutron states. As shown in Fig. 3, the 2^- state of an $s_{1/2}$ orbital neutron is calculated around the ${}^9\text{Li}-n$ threshold. Recently, we applied the Jost function method to the effective ${}^9\text{Li}-n$ potential derived from the CC calculation, and obtained a virtual state for the s -wave neutron.⁴⁾ This result indicates that the CC calculation including the Pauli blocking effect reproduces a level inversion of $s_{1/2}$ - and $p_{1/2}$ -neutron orbits.

The results of s - and d -wave solutions in CC imply that the effective ${}^9\text{Li}-n$ potential for s - and d -waves is more attractive than that for the $p_{1/2}$ -wave neutron. It is explained by the Pauli blocking of the pairing correlation in the ${}^9\text{Li}$ core due to the appearance of the $p_{1/2}$ -orbit neutron in the interaction region of the ${}^{10}\text{Li}$ ($= {}^9\text{Li}+n$) system. In Fig. 4, we display the effective ${}^9\text{Li}-n$ potentials V_{eff} for $p_{1/2}$ -, $s_{1/2}$ - and d -wave neutrons, where ΔV_{Pauli} is the Pauli blocking repulsive potential and V^F is the single channel folding potential. We see that the Pauli blocking repulsive potential is very strong in the interior region between ${}^9\text{Li}$ and the $p_{1/2}$ -wave neutron, but contributes very weakly and negligibly to the s - and d -wave neutrons, respectively. Thus, the effective potential for ${}^9\text{Li}+n$ is expressed approximately as

$$V_{\text{eff}}^p \approx V^F + \Delta V_{\text{Pauli}}^p \quad \text{for } p\text{-orbit}, \quad (4.6)$$

$$V_{\text{eff}}^{s,d} \approx V^F \quad \text{for } s\text{- and } d\text{-orbits}. \quad (4.7)$$

From these results, it is also concluded that the $p_{1/2}$ -orbital resonances are pushed up due to the Pauli blocking repulsive effect by an amount equal to the energy loss due to the breaking of the pairing correlation.

4.2. Halo structure of ${}^{11}\text{Li}$

We also solve the three-body problem of the ${}^9\text{Li}+n+n$ system with the coupled-channel OCM, where multi-configurations are taken into account for the ${}^9\text{Li}$ core. The wave function of ${}^{11}\text{Li}$ is expressed as;

$$\Psi({}^{11}\text{Li}) = \sum_i \mathcal{A}\{\Phi(C_i)\chi_i(\vec{r}_1, \vec{r}_2)\}, \quad (4.8)$$

where, $\chi_i(r_1, r_2)$ describes the wave function of two valence neutrons around the ${}^9\text{Li}$ core C_i . This wave function $\chi_i(r_1, r_2)$ is solved from the following equation:

$$\sum_{j=0}^2 [\{T_c + T_{n_1} + T_{n_2} - T_{cm} + V_{cn_1} + V_{cn_2} + v_{nn} + \lambda(\Lambda_j(n_1) + \Lambda_j(n_2))\} \delta_{ij} + h_{ij}({}^9\text{Li})] \chi_j(\vec{r}, \vec{r}_2) = E\chi_i(\vec{r}_1, \vec{r}_2). \quad (i = 0, 1, 2) \quad (4.9)$$

We solve this coupled channel OCM equation of ${}^9\text{Li}+n+n$ in the similar way as ${}^4\text{He}+n+n$ by using the hybrid-TV model. Here, we discuss important couplings between ${}^9\text{Li}$ and valence neutrons in the ${}^{11}\text{Li}$ ground state, which are shown in Fig. 5. We classify the state of ${}^{11}\text{Li}$ by three kinds of configurations (a), (b) and (c), where

shaded area shows the part of ${}^9\text{Li}$. (a) is the lowest p -shell closed configuration, (b) configurations of two valence neutrons excited in the higher orbits, and (c) configurations of two valence neutrons the same as those of (b) and $2p-2h$ of the ${}^9\text{Li}$ core due to the neutron pairing correlation. In the calculation, these configurations are coupled through the pairing interaction G_{pair} which can be separated into the following terms;

$$G_{\text{pair}} = G_{\text{core}} + G_{\text{val}} + G_{\text{core-val}}, \quad (4.10)$$

where G_{core} is the pairing interaction appeared in $h_{ij}({}^9\text{Li})$ for the ${}^9\text{Li}$ part. G_{val} is the pairing matrix element between valence neutrons, where the Minnesota interaction is used. $G_{\text{core-val}}$ produces the coupling which expresses the exchange effect of two neutron-pairs between that in ${}^9\text{Li}$ and valence ones. In ${}^{10}\text{Li}$, such a neutron-pair exchange term does not appear.

When we employ the effective ${}^9\text{Li}$ - n interaction which reproduces virtual s -waves as discussed above, we obtain a too large binding energy (-2.6 MeV) for ${}^{11}\text{Li}$. The reason is that the Pauli-blocking on the pairing interaction in ${}^9\text{Li}$ works only once even if two valence neutrons are added. On the other hand, the attractive ${}^9\text{Li}$ - n interaction works twofold in ${}^{11}\text{Li}$. Furthermore, the $(s_{1/2})^2$ component of the valence neutrons is very small (2 %) in the obtained ${}^{11}\text{Li}$ wave function. These results indicate that we need to consider other effects in ${}^{11}\text{Li}$ in addition to the Pauli blocking effect in order to obtain a consistent understanding for ${}^{10}\text{Li}$ and ${}^{11}\text{Li}$.

In our model, the radial distribution of neutrons in the ${}^9\text{Li}$ core is described by a Gaussian form obtained from the

HO wave functions assumed for an isolated ${}^9\text{Li}$ nucleus. However, a very long range part of the ${}^9\text{Li}$ - n interaction may play an important role in weak binding systems such as ${}^{10}\text{Li}$ and ${}^{11}\text{Li}$. Since the long range part of interaction is proportional to an exponential density distribution, we may have to modify the tail part of the folding ${}^9\text{Li}$ - n interaction by adding a Yukawa form $-v_t \frac{e^{-r/b_t}}{r}$. We here employ a range parameter $b_t=2.4$ fm to fit the neutron separation energy of ${}^9\text{Li}$. The strength v_t is varied as 40, 55 and 65 MeV. In Fig. 6, we show the modification of the tail part in the ${}^9\text{Li}$ - n interaction. In addition of the tail effect, it is expected that matrix element of $\langle (0p)^2 | v_{nn} | (1s)^2 \rangle$ may be changed due to the exchange between two neutron-pairs in the ${}^9\text{Li}$ core and of the valence part. If valence neutrons are in $1s_{1/2}$ orbits, through the exchange between valence neutrons and the p -orbit neutrons in the ${}^9\text{Li}$ core, valence neutrons cannot be distinguished from those in $0p$ -orbits. Such

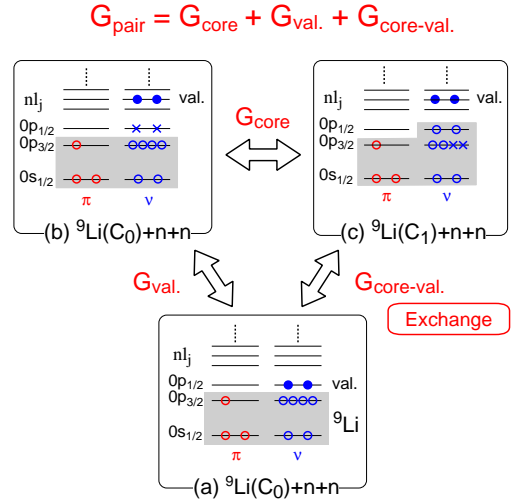


Fig. 5. Coupling scheme in ${}^{11}\text{Li}$ through the pairing interaction G between two neutrons in ${}^9\text{Li}$ and valence neutrons.

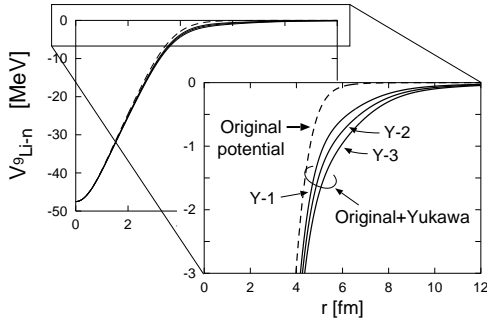


Fig. 6. ${}^9\text{Li}$ - n potential including tail effect.

an effect is expressed effectively as an enhancement of $\langle(0p)^2|v_{nn}|(1s)^2\rangle$.

Using the ${}^9\text{Li}$ - n interaction including these effects, we calculate the ground state of ${}^{11}\text{Li}$ and the obtained result is shown in Table I. Y-1, Y-2, and Y-3 correspond to the parameter sets of $v_t = 40, 50,$ and 65 MeV, respectively. The parameter α_{s-p} given in Table I expresses the enhancement of $(0p)^2$ - $(1s)^2$ pairing coupling as; $\langle(0p)^2|v_{nn}|(1s)^2\rangle \rightarrow \alpha_{s-p} \cdot \langle(0p)^2|v_{nn}|(1s)^2\rangle$.

As shown in Table I, every parameter set reproduces the observed binding energy 0.3 MeV of ${}^{11}\text{Li}$. The $(s_{1/2})^2$ amplitude of the halo wave function strongly depends on the tail parameters for the mean field potential. The matter radius also depends on the $(s_{1/2})^2$ amplitude. It is very interesting to see the excited structure based on the success of the ground state properties obtained here.

§5. Coulomb breakup in the complex scaling method

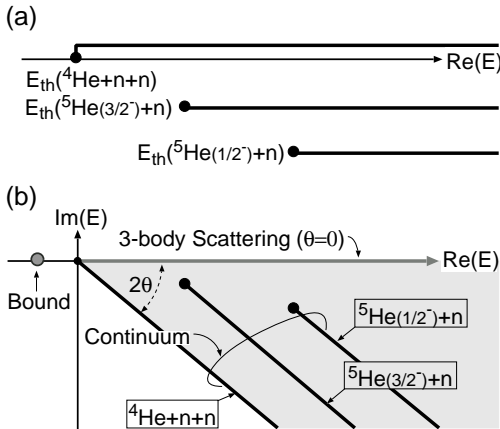


Fig. 7. (a) ${}^4\text{He}+n+n$ and $[{}^4\text{He}+n]_{\text{res}}+n$ thresholds and continua in ${}^6\text{He}$ on the complex energy plane. (b) The complex scaled continua in the complex scaling method.

Table I. Results of ${}^{11}\text{Li}$ within the Pauli-blocking and the mean field effect. Unit in MeV for energy and fm for matter radius.

	Y-1	Y-2	Y-3
B.E. [MeV]	0.31	0.31	0.31
$P(s^2)$	9.8%	18.5%	26.0%
R_m [fm]	3.00	3.21	3.47
α_{s-p}	2.3	2.6	2.8

In Fig. 2, we showed resonant states in addition to the ground state in ${}^6\text{He}$, which are obtained by applying the complex scaling method⁶⁾ to the ${}^4\text{He}+n+n$ three-cluster model. In the complex scaling method, continuum solutions are also obtained along the rotated cuts. We show a schematic diagram of the rotated cuts for the ${}^4\text{He}+n+n$ system in Fig. 7. We can see three kinds of rotated cuts: ${}^4\text{He}+n+n$ three-body, ${}^5\text{He}(3/2^-)+n$ quasi-two-body and ${}^5\text{He}(1/2^-)+n$ quasi-two-body cuts, which are degenerating into a single line of the real energy axis for $\theta = 0$. For the complex scaled solutions of bound states, resonances and continuum states, we apply the extended complete-

ness relation: 7), 8)

$$\sum_B |\Psi_B^\theta\rangle \langle \tilde{\Psi}_B^\theta| + \sum_R^{N_\theta} |\Psi_R^\theta\rangle \langle \tilde{\Psi}_R^\theta| + \int dE_\theta |\Psi_{k_\theta}\rangle \langle \tilde{\Psi}_{k_\theta^*}| = 1, \quad (5.1)$$

where N_θ is a number of resonance solutions obtained for the θ -rotated Hamiltonian, and E_θ are complex energies taken along the 2θ -lines of the rotated energy axes.

For an external field described by the operator \hat{O} , the strength function $F(E)$ is calculated as

$$F(E) = \sum_\nu \langle \Psi_{gr} | \hat{O}^\dagger | \Psi_\nu \rangle \langle \tilde{\Psi}_\nu | \hat{O} | \Psi_{gr} \rangle \delta(E - E_\nu) = -\frac{1}{\pi} \text{Im}R(E). \quad (5.2)$$

Here, $R(E)$ is the so-called response function defined by

$$R(E) = \int dr dr' \tilde{\Psi}_{gr}^*(r) \hat{O}^\dagger G(r, r') \hat{O} \Psi_{gr}(r'). \quad (5.3)$$

By using the complex scaling method, this response function is calculated as

$$R(E) = \int dr dr' \tilde{\Psi}_{gr}^*(re^{-\theta}) \hat{O}^\dagger (re^\theta) G^\theta(r, r') \hat{O} (re^\theta) \Psi_{gr}(r'e^\theta), \quad (5.4)$$

where Green's function is calculated by using the extended completeness relation, Eq. (5.1), as

$$\begin{aligned} G^\theta(r, r') = & \sum_B \frac{\Psi_B(r, k_B) \tilde{\Psi}_B^*(r', k_B)}{E - E_B} + \sum_R^{N_\theta} \frac{\Psi_R(r, k_R) \tilde{\Psi}_R^*(r', k_R)}{E - E_R} \\ & + \int dE_\theta \frac{\Psi(r, k_\theta) \Psi^*(r', k_\theta^*)}{E - E_\theta}. \end{aligned} \quad (5.5)$$

Inserting this form of Green's function into Eq. (5.2), we obtain the strength function separated into three terms of bound-state, resonant-state and continuum-state contributions:

$$F(E) = F_B(E) + F_R^\theta(E) + F_k^\theta(E), \quad (5.6)$$

where separation of resonances and continua depends on the scaling angle θ .

We calculate the Coulomb dissociation cross section by using $E1$ and $E2$ transition strengths obtained above. The cross section is expressed by multiplying the reduced transition probability $dB(E\lambda, E)/dE$ and the virtual photon number $N_{E\lambda}(E)$ from the equivalent photon method.²⁰⁾ In Fig. 8, we show the calculated cross section in comparison with the experimental one,²¹⁾ where the target is Pb and the incident energy of ${}^6\text{He}$ projectile is 240 MeV/nucleon. In this calculation, the minimum value of the impact parameter is 12 fm. We also calculate the convoluted cross section in addition to the original one. The parameter set for the convolution with respect to the energy resolution and the detector response is the same as that used by Aumann et al.²¹⁾

The entire shape of our cross section is very similar to the experimental data except for the extremely large peak at around 1 MeV, which mainly comes from

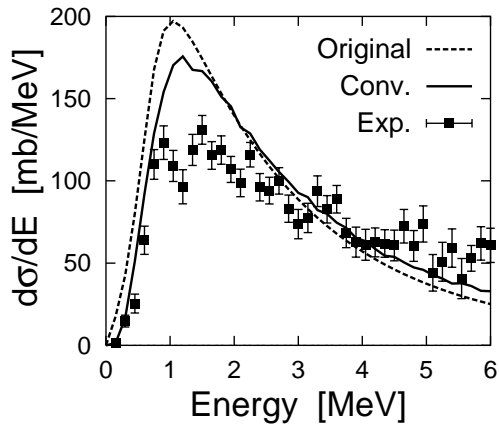


Fig. 8. Coulomb dissociation cross sections of ${}^6\text{He}$ into the ${}^4\text{He}+n+n$ system with and without the convolution. Experimental data are taken from Aumann et al.²¹⁾

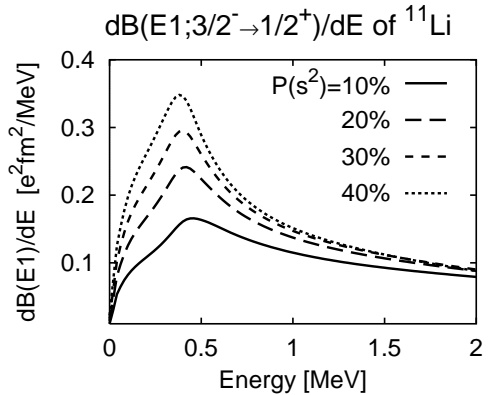


Fig. 9. $E1$ transition strength from the ground state ($3/2^-$) of ${}^{11}\text{Li}$ to continuum states ($1/2^+$). The distributions are shown for the calculated ground state wave functions which have various values of $(s_{1/2})^2$ amplitudes.

the $E1$ component. It is found that the $E2$ component is quite small and that its structure cannot be seen in the total cross section even if there is a 2_1^+ resonance.

In Fig. 9, we show the $E1$ strength distribution of ${}^{11}\text{Li}$, which is obtained by applying the present method to the multi-configuration ${}^9\text{Li}+n+n$ model presented in the previous section.

§6. Summary and conclusion

We proposed a new model of core+neutrons in which degrees of freedom in the core cluster are taken into consideration on an equal footing with the weakly-binding motion of valence neutrons. The coupling between these degrees of freedom was solved by employing OCM to treat the antisymmetrization.

It was discussed that such a dynamical coupling is very important in ${}^{10}\text{Li}$ and ${}^{11}\text{Li}$ but less important in ${}^6\text{He}$. The coupling in ${}^6\text{He}$ can be treated in a perturbative way in the ${}^4\text{He}+n+n$ model. However, the couplings in ${}^{10}\text{Li}$ and ${}^{11}\text{Li}$ are shown to have to be solved explicitly by using coupled channel frameworks, where the Pauli principle between valence and core neutrons plays an important role. We here took the pairing correlation as an important degree of freedom in the core cluster.

It was shown that the Pauli blocking effect can explain a degeneracy of p - and s -orbital energies in the spectroscopy of ${}^{10}\text{Li}$. The ${}^9\text{Li}-n$ interaction is shown to have a strong state dependence which works more attractively for s -orbit than for p -orbit. However, in ${}^{11}\text{Li}$, it was shown that, in addition to the Pauli blocking effect on the pairing correlation in the ${}^9\text{Li}$ core, a spatially extend tail of the ${}^9\text{Li}-n$ potential is needed to reproduce a large amplitude of s -wave valence neutron configurations. Taking these effects, we can explain the properties of ${}^{10}\text{Li}$ and ${}^{11}\text{Li}$ consistently.

After this conference, we received a recent experimental result on ${}^{10}\text{Li}$,²²⁾ which

suggests 1^+ and 2^+ resonances at lower energies. Based on their new data, we recalculated the present model. The preliminary results indicate that the present qualitative conclusions are not changed though quantitative values of some parameters are a little shifted from the present ones.

The complex scaling method has been used as a powerful method to solve resonances of three-body systems without any troubles with asymptotic boundary conditions. In addition to resonance solutions in the complex scaling method, we showed that continuum states play an important role in the description of unbound three-body systems. This fact is proven by extending the completeness relation for the complex scaled Hamiltonian. We applied this new approach to $^4\text{He}+n+n$ and $^4\text{Li}+n+n$ systems, and discussed the Coulomb breakup cross section of ^6He in comparison with experiments. Through the calculated strength distribution, we can obtain much interesting information about the unbound structure and the breakup reaction mechanism.

Acknowledgements

The authors would like to thank H. Masui and T. Yamada for useful discussions.

References

- 1) S. Aoyama, S. Mukai, K. Katō and K. Ikeda, *Prog. Theor. Phys.* **93** (1995), 99; *ibid.* **94** (1995), 43.
- 2) S. Mukai, S. Aoyama, K. Katō and K. Ikeda, *Prog. Theor. Phys.* **99** (1998), 381.
- 3) K. Katō, T. Yamada and K. Ikeda, *Prog. Theor. Phys.* **101** (1999), 119.
- 4) H. Masui, S. Aoyama, T. Myo, K. Katō and K. Ikeda, *Nucl. Phys. A* **673** (2000), 207.
- 5) M. V. Zhukov, B. V. Danilin, D. F. Fedorov, J. M. Bang, I. J. Thompson and J. S. Vaagen, *Phys. Rep.* **231** (1993), 151.
- 6) J. Aguilar and J. M. Combes, *Commun. Math. Phys.* **22** (1971), 269.
E. Balslev and J. M. Combes, *Commun. Math. Phys.* **22** (1971), 280.
- 7) T. Myo, A. Ohnishi and K. Katō, *Prog. Theor. Phys.* **99** (1998), 801.
- 8) T. Myo, S. Aoyama, K. Katō and K. Ikeda, *Phys. Rev. C* **63** (2001), 054313.
- 9) I. Tanihata et al., *Phys. Rev. Lett.* **55** (1985), 2676.
- 10) I. Tanihata, *Nucl. Phys. A* **488** (1988), 113c.
- 11) I. Tanihata, *J. of Phys. G* **22** (1996), 157.
- 12) S. Saito, *Prog. Theor. Phys. Suppl. No. 62* (1977), 11.
- 13) Y. Suzuki and K. Ikeda, *Phys. Rev. C* **38** (1988), 410.
Y. Suzuki and Wang Jing Ju, *Phys. Rev. C* **41** (1990), 736.
- 14) Y. Tosaka, Y. Suzuki and K. Ikeda, *Prog. Theor. Phys.* **83** (1990), 1140.
- 15) K. Ikeda, *Nucl. Phys. A* **538** (1992), 355c.
- 16) H. Kanada, T. Kaneko, S. Nagata and M. Nomoto, *Prog. Theor. Phys.* **61** (1979), 1327.
- 17) Y. C. Tang, M. LeMere and D. R. Thompson, *Phys. Rep.* **47** (1978), 167.
- 18) H. G. Bohlen et al., *Z. Phys. A* **344** (1993), 381.
- 19) K. Katō and K. Ikeda, *Prog. Theor. Phys.* **89** (1993), 623.
- 20) B. Hoffmann and G. Baur, *Phys. Rev. C* **30** (1984), 247.
C. A. Bertulani and G. Baur, *Phys. Rep.* **163** (1988), 299.
- 21) T. Aumann et al., *Phys. Rev. C* **59** (1999), 1252.
- 22) H. G. Bohlen et al., *Z. Phys. A* **344** (1993), 381.